

## Photogeneration of reactive oxygen species by 3-arylcoumarin and flavanocoumarin derivatives

M. Rajendran<sup>a</sup>, J. Johnson Inbaraj<sup>b</sup>, R. Gandhidasan<sup>c</sup>, R. Murugesan<sup>c,\*</sup>

<sup>a</sup> Department of Chemistry, NMSSVN College, Madurai 625 019, Tamilnadu, India

<sup>b</sup> Department of Chemistry & Biochemistry, Hughes Laboratories, Miami University, Oxford, OH 45056, USA

<sup>c</sup> School of Chemistry, Madurai Kamaraj University, Madurai 625 021, Tamilnadu, India

Received 25 July 2005; received in revised form 10 January 2006; accepted 17 January 2006

Available online 28 February 2006

### Abstract

The photodynamic properties of six 3-arylcoumarins, viz., 3-phenyl-4-hydroxycoumarin (AC1), 3-phenyl-4-methoxycoumarin (AC2), 3-(4-methoxyphenyl)-4-hydroxycoumarin (AC3), 3-(4-methoxyphenyl)-4-methoxycoumarin (AC4), 3-(3',4'-methylenedioxyphenyl)-4-hydroxycoumarin (AC5), 3-(3',4'-methylenedioxyphenyl)-4-methoxycoumarin (AC6) and four flavanocoumarins viz., 2-(3-coumaryl)-7-methoxy-3-phenylchromone (FC I), 2-(3-coumaryl)-7-methoxy-3-(4-methoxy)phenylchromone (FC II), 2-(3-coumaryl)-5,7-dimethoxy-3-phenylchromone (FC III) and 2-(3-coumaryl)-5,7-dimethoxy-3-(4-methoxy)phenyl chromone (FC IV) are studied. The photogeneration of  $^1\text{O}_2$  is followed by *N,N*-dimethyl-4-nitrosoaniline (RNO) bleaching and EPR–TEMPL (2,2,6,6-tetramethyl piperidinol) methods. Relative to rose bengal, singlet oxygen generating efficiencies of AC1, AC2, AC3, AC4, AC5 and AC6 are found to be 0.113, 0.079, 0.043, 0.028, 0.045 and 0.083, respectively. Similarly of FC I, FC II, FC III and FC IV are found to be 0.04, 0.03, 0.10 and 0.06 respectively. The photogeneration of  $\text{O}_2^{\bullet-}$  is monitored by optical spectroscopy using SOD-inhibitable cytochrome *c* reduction assay and by EPR spin trapping method using the spin trap, 5,5-dimethyl-1-pyrroline-*N*-oxide (DMPO). Photogeneration of  $\text{O}_2^{\bullet-}$  radical is effectively enhanced by electron donors. Our results indicate that 3-arylcoumarin and flavanocoumarin derivatives possess only moderate ability to generate  $^1\text{O}_2$  and  $\text{O}_2^{\bullet-}$ . Both Type I and Type II paths are involved in the photodynamic action of 3-arylcoumarins as well as of flavanocoumarins.

© 2006 Elsevier B.V. All rights reserved.

**Keywords:** 3-Arylcoumarins; Flavanocoumarins; Singlet oxygen; Superoxide anion

### 1. Introduction

Coumarins (also known as benz- $\alpha$ -pyrone) are compounds consisting of fusion of benzene and  $\alpha$ -pyrone rings. Physiologic, pharmacologic, phototoxic and photoallergic properties of coumarin derivatives are well-documented [1,2]. Coumarins also show antiviral [3] and antifungal [4] properties. Alkyl or alkoxy substituted coumarins are found to exhibit photosensitising properties. Also, the substitution of methoxy or ethoxy group at coumarin nucleus increases the phototoxicity [5]. Coumarins, furanocoumarins and thiocoumarins are also found to act as photosensitisers in relation to the generation of singlet oxygen. Pyrrolocoumarins are found to have photohaemolytic activity but not phototoxic on guinea pig skin [6].

The treatment for vitiligo and psoriasis by oral administration of 8-methoxypsoralen followed by exposure to UV light A, is well-documented [7]. Photodynamic effects induced on a membrane system by furocoumarins show photodamage to isolated mitochondria [8–10]. The photodynamic action of furocoumarins (psoralens) appears to involve activated oxygen species ( $^1\text{O}_2$ ,  $\text{O}_2^{\bullet-}$  and  $\bullet\text{OH}$ ) [11]. A kinetic analysis of 8-methoxy-psoralens sensitised photooxidation of cystein and reduced glutathione supports the involvement of singlet oxygen mechanism. [12]. Flavanocoumarins are compounds in which coumarin ring is fused in the 2-position of the chromone moiety. Because of the presence of coumarin and chromone rings, flavanocoumarins may exhibit enhanced activity.

Because of the current interest in the photogeneration of ROS by coumarin derivatives, this paper reports the photogeneration of ROS from 3-arylcoumarin derivatives and flavanocoumarins. The results demonstrate that 3-arylcoumarins and flavanocoumarins have moderate potential to photogenerate

\* Corresponding author. Tel.: +91 452 2458471; fax: +91 452 459105.  
E-mail address: [rammurugesan@yahoo.com](mailto:rammurugesan@yahoo.com) (R. Murugesan).

ROS. The effect of electron donors such as ethylenediaminetetraacetic acid (EDTA) and reduced nicotinamide adenine dinucleotide (NADH) on the rate of production of ROS by these 3-aryl coumarins and flavanocoumarins is also investigated.

## 2. Experimental section

### 2.1. Chemicals

Superoxide dismutase (SOD), catalase and cytochrome *c* were purchased from Sigma Chemical Co., while reduced nicotinamide adenine dinucleotide (NADH) was obtained from Boehringer, Mannheim. *N,N*-Dimethyl-4-nitrosoaniline (RNO), 1,4-diazabicyclo-[2,2,2]octane (DABCO), diethyltriaminopentaacetic acid (DETAPAC), and rose bengal (RB) were obtained from Aldrich. The spin trap, DMPO was obtained from Aldrich and was purified by activated charcoal method [13]. 2,2,6,6-Tetramethyl piperidinol (TEMPL) was obtained from Merck, India. Imidazole, ethylenediamine-tetraacetic acid (EDTA) and sodium azide were purchased from S.D. Fine Chemicals, India. Imidazole was used after repeated crystallisation from doubly distilled water. All other compounds were used as received.

### 2.2. Arylcoumarins

The chemical structures of the 3-arylcoumarins studied are given in Fig. 1. These arylcoumarins 3-phenyl-4-hydroxycoumarin (AC1), 3-phenyl-4-methoxycoumarin (AC2), 3-(4-methoxyphenyl)-4-hydroxycoumarin (AC3), 3-(4-methoxyphenyl)-4-methoxycoumarin (AC4), 3-(3',4'-methylenedioxyphenyl)-4-hydroxycoumarin (AC5), and 3-(3',4'-methylenedioxyphenyl)-4-methoxycoumarin (AC6) were received as gift from the department of natural products chemistry, Madurai Kamaraj University, Madurai, India.

### 2.3. Flavanocoumarins

#### 2.3.1. Synthesis of 3-aryl-2-(3-coumaryl)chromone

Flavanocoumarins were prepared following the reported procedure [14], by refluxing equimolar amounts of the corresponding benzyl-2-hydroxyphenyl ketones (5 mM) and coumarin-3-carboxylic acid chloride (5 mM) in the presence of organic base like pyridine (6 ml) for 4 h. After the reaction was complete, the reaction mixture was poured into ice-cold water and the resulting solid was filtered and crystallised from alcohol.

2-(3-Coumaryl)-7-methoxy-3-phenylchromone (FC I) was prepared according to the general procedure given above using benzyl-2-hydroxy-4-methoxyphenyl ketone and coumarin-3-carboxylic acid chloride as the starting materials. Upon recrystallisation from alcohol pale yellow crystals of FC I were obtained (m.p. 254–255 °C). NMR (CDCl<sub>3</sub>): 3.92 (s, 3H, OCH<sub>3</sub>), 6.68 (d, 1H, H-8), 7.10 (dd, 1H, H-6), 7.24–7.34 (m, 7H, H-8', 6', 2'', 3'', 5'', 6''), 7.38 (dd, 1H, H-7'), 7.57 (m, 1H, H-5'), 7.65 (s, 1H, H-4'), 8.19 (d, 1H, H-5).

2-Hydroxy-4-methoxyphenyl-4-methoxybenzyl ketone was condensed with coumarin-3-carboxylic acid chloride for the synthesis of 2-(3-coumaryl)-7-methoxy-3-(4-methoxy)phenylchromone (FC II) (m.p. 150–152 °C). NMR (CDCl<sub>3</sub>):

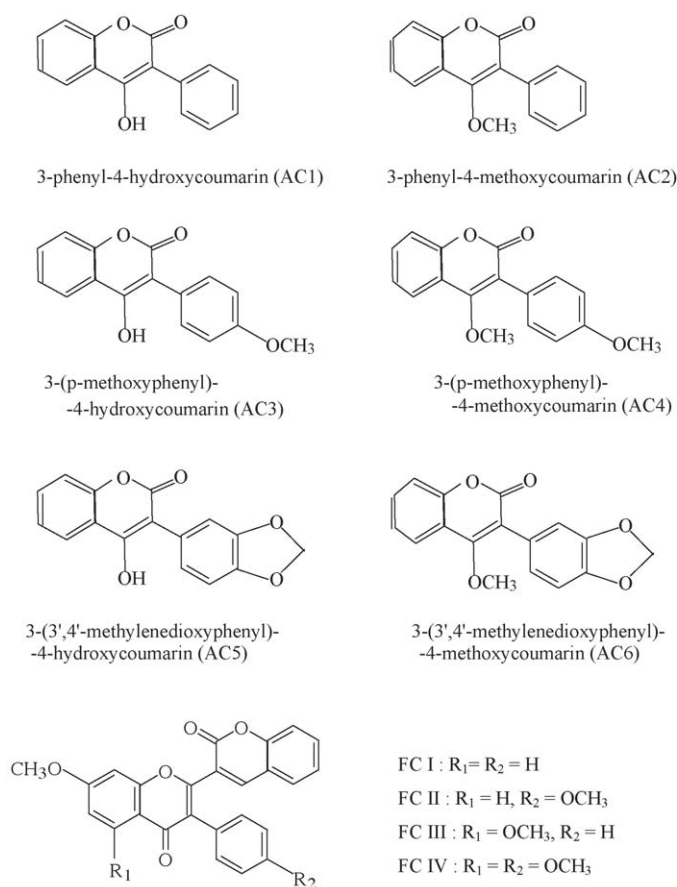


Fig. 1. Chemical structures of 3-arylsubstituted coumarins and flavanocoumarins.

3.77 (s, 3H, OCH<sub>3</sub>), 3.91 (s, 3H, OCH<sub>3</sub>), 6.84 (d, 2H, H-3'', 5''), 6.88 (d, 1H, H-8), 6.68 (dd, 1H, H-6), 7.25 (d, 2H, H-2'', 6''), 7.29 (d, 1H, H-8'), 7.31 (d, 1H, H-6'), 7.40 (dd, 1H, H-7'), 7.58 (m, 1H, H-5'), 7.74 (s, 1H, H-4'), 8.15 (d, 1H, H-5).

2-(3-Coumaryl)-5,7-dimethoxy-3-phenylchromone (FC III) was synthesised by using benzyl-2-hydroxy-4,6-dimethoxyphenyl ketone and coumarin-3-carboxylic acid chloride as starting materials. On recrystallisation from alcohol, FC III was obtained as colourless crystals (m.p. 218–220 °C). NMR (CDCl<sub>3</sub>): 3.90 (s, 3H, OCH<sub>3</sub>), 6.40 (d, 1H, H-8), 6.50 (d, 1H, H-6), 7.21–7.38 (m, 8H, H-6', 7', 2'', 3'', 4'', 5'', 6''), 7.59 (m, 1H, H-5'), 7.64 (s, 1H, H-4').

2-(3-Coumaryl)-5,7-dimethoxy-3-(4-methoxy)phenyl chromone (FC IV) was prepared from 2-hydroxy-4,6-dimethoxyphenyl-4-methoxybenzyl ketone and coumarin-3-carboxylic acid chloride (m.p. 255–257 °C). NMR (CDCl<sub>3</sub>): 3.75 (s, 3H, OCH<sub>3</sub>), 3.89 (s, 3H, OCH<sub>3</sub>), 3.98 (s, 3H, OCH<sub>3</sub>), 6.38 (d, 1H, H-8), 6.48 (d, 1H, H-6), 6.80 (d, 2H, H-3'', 5''), 7.24 (d, 2H, H-2'', 6''), 7.27 (d, 1H, H-8'), 7.32 (d, 1H, H-6'), 7.39 (dd, 1H, H-7'), 7.57 (m, 1H, H-5'), 7.68 (s, 1H, H-4'). The chemical structures of these flavanocoumarins are given in Fig. 1.

### 2.4. Photostability of coumarin derivatives

Photostability of 3-arylcoumarins and flavanocoumarins was examined by measuring UV absorption spectra in DMSO

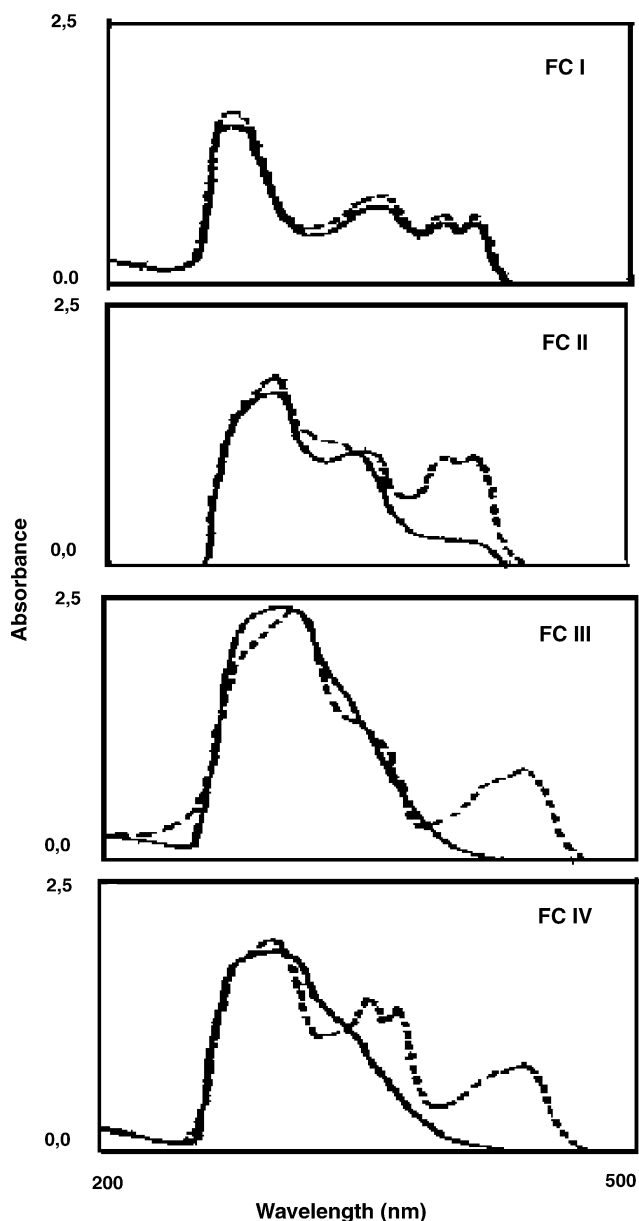


Fig. 2. UV absorption spectra of flavanocoumarins before (solid line) and after (dashed line) irradiation for 3 min, using 150 W xenon lamp, with water filter to cut off infrared radiation.

before and after irradiation for a given period of time. The absorption spectra of flavanocoumarins observed before and after irradiation for 3 min are given in Fig. 2. Upon irradiation, two new peaks appeared in the range of 350–440 nm and their intensity increased with irradiation time, suggesting that flavanocoumarins undergo photodegradation, producing a new chromophore with absorption at longer wavelengths. But, absorption spectra of the 3-arylcoumarin derivatives did not show any change on irradiation (figure not shown), indicating greater photostability.

## 2.5. Light source

Light source used for irradiation was a 150 W xenon lamp. A filter combination of 10 cm potassium iodide solution (1 g in

100 ml) and 1 cm pyridine was used to cut off below 300 nm and to achieve a spectral window of 300–700 nm. The reaction mixture in a quartz cuvette, placed at a distance of 12 cm from the light source was continuously stirred during irradiation.

## 2.6. Optical spectroscopy

### 2.6.1. RNO bleaching assay

The generation of  $^1\text{O}_2$  was measured by an indirect chemical method, utilizing imidazole and RNO [15]. Optical measurements were done using either a Shimadzu UV-VIS spectrometer (UV-160) or using Specord S 100 UV-VIS spectrometer, Analytik Jena AG, Jena, Germany. The sensitizers were exposed to light in the presence of imidazole (10 mM) and RNO (50 mM) in phosphate buffer (pH 7.4).  $^1\text{O}_2$  formed by energy transfer from the photoexcited 3-arylcoumarin/flavanocoumarin derivatives reacts with imidazole to form transannular peroxide, which bleaches RNO, and the bleaching was monitored spectrophotometrically at 440 nm. For additional support for the formation of  $^1\text{O}_2$ , the RNO bleaching was studied in the presence of  $^1\text{O}_2$  quenchers. The rate of disappearance of quencher obeys first order kinetics and the slope of the first order plot was calculated as described earlier [16]. Each compound under investigation along with the reference singlet generator, RB was studied under identical conditions. The relative ratio of the slopes of the 3-arylcoumarins and RB, after correction for molar absorption and photon energy [17] was used to compute the relative efficiency of singlet oxygen generation taking  $\Phi(^1\text{O}_2)=0.76$  for RB [18]. Contribution of  $\text{O}_2^{\bullet-}$  and  $\text{H}_2\text{O}_2$  in the RNO bleaching was eliminated by the addition of SOD and catalase.

### 2.6.2. SOD-inhibitable cytochrome *c* reduction assay

Photogeneration of  $\text{O}_2^{\bullet-}$  was detected by using the SOD-inhibitable cytochrome *c* reduction method [19]. 3-Arylcoumarins/flavanocoumarin were photolysed in the presence of ferricytochrome *c* (40  $\mu\text{M}$ ) in 50 mM phosphate buffer (pH 7.4). The reduction was followed by observing the increase in 550 nm absorption peak of cytochrome *c* as a function of irradiation time [20].

## 2.7. EPR spectroscopy

### 2.7.1. DMPO-spin trapping method

The EPR DMPO-spin trapping experiments were carried out using JEOL JES-TE100 X-BANDESR spectrometer. The irradiated samples were drawn into a gas-permeable Teflon capillary tube (Zeus Industries, Orangeburg, SC, USA). Each capillary was folded twice, inserted into a narrow quartz tube open on both sides and then placed in the EPR cavity. The following parameters were used for EPR measurements: microwave power, 2 mW; modulation frequency, 100 kHz; modulation amplitude, 0.5 G.

Solutions of 3-arylcoumarin (0.4 mM)/flavanocoumarin (0.1 mM) were irradiated in the presence of DMPO (100 mM), in DMSO and the EPR spectra were recorded at different intervals of irradiation time. The transient radical species were trapped by DMPO to form DMPO-spin adducts. The spectral identification of the spin-adducts were confirmed by independently simulat-

ing the spectra with known hyperfine coupling constants (hfccs) and comparing them with the experimentally observed ones.

### 2.7.2. EPR–TEMPL method

The optical RNO bleaching method has a limitation, because coumarins and RNO absorb in the same region. Hence another technique, the EPR–TEMPL method was also used to study the formation of  $^1\text{O}_2$  [21,22]. Photogenerated  $^1\text{O}_2$  reacts with TEMPL, leading to the paramagnetic TEMPOL, which shows a characteristic three line EPR spectrum. Reaction mixture (1 ml) containing 0.02 M TEMPL and 0.2 mM of 3-arylcoumarins/flavanocoumarins was irradiated and the increase in EPR signal intensity of TEMPOL was followed as a function of irradiation time.

## 3. Results and discussion

### 3.1. Photodynamic action of 3-arylcoumarins

#### 3.1.1. Energy transfer process

The loss of RNO absorbance at 440 nm, as a function of irradiation time, for AC1–AC6 is shown in Fig. 3. 3-Arylcoumarins show first order plot except AC6 and AC2. These two coumarins generate larger amount of  $^1\text{O}_2$ , which on reaction with  $\text{O}_2$ . Since the dissolved oxygen in the cell may be depleted, saturating profile curves are obtained for AC6 and AC2. But  $^1\text{O}_2$  yields were calculated according to first order kinetics. Photobleaching of RNO by 3-arylcoumarins was observed neither in dark nor in the absence of  $\text{O}_2$  and light. The ratio of the slope of RB to 3-arylcoumarins was corrected for molar absorption and photon energy to obtain the singlet oxygen generating efficiencies of the 3-arylcoumarins [23]. After this correction, the  $^1\text{O}_2$  yields were found to be 0.113, 0.083, 0.079, 0.045, 0.043 and 0.028 for AC1, AC6, AC2, AC5, AC3 and AC4, respectively, taking  $\Phi(^1\text{O}_2)$  of RB = 0.76. In Fig. 3 the compounds AC2 and AC5

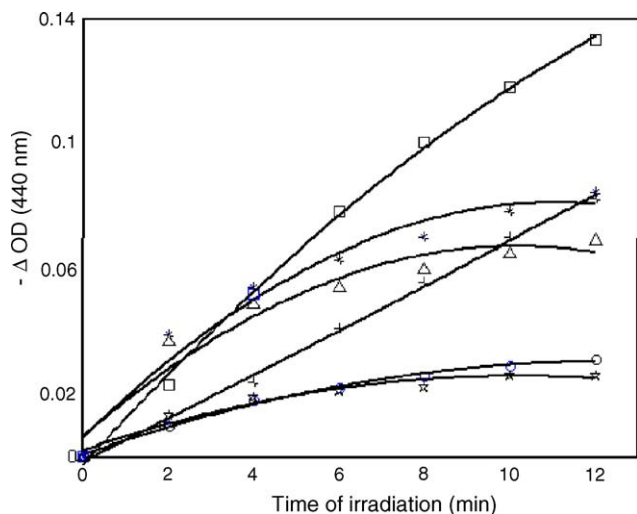


Fig. 3. Photosensitized RNO bleaching, measured at 440 nm, as a function of irradiation time in the presence of imidazole (10 mM) in 50 mM phosphate buffer (pH 7.4) by AC1 (□□□), AC2 (△△△), AC3 (○○○), AC4 (○○○), AC5 (xxx) and AC6 (\*\*\*)

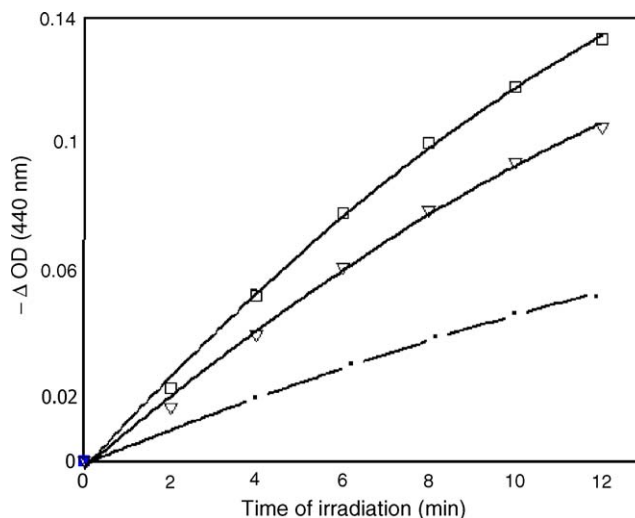
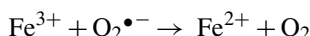


Fig. 4. The effect of sodium azide (0.1 mM) (●●●) and DABCO (5 mM) (▽▽▽) on the bleaching of RNO for photosensitisation with AC1 (□□□) in the presence of imidazole (10 mM) in phosphate buffer (pH 7.4).

show the change at irradiation time 0. This type of observation is not an experimental error. The changes are not observed at zero time in absorbance. But in order to fit the experimental points we are using curve-fitting method so that it looks like change at zero irradiation time.

To support the photogeneration of  $^1\text{O}_2$ , experiments were carried out in the presence of specific singlet oxygen quenchers. The singlet oxygen quenching rate constants of DABCO ( $1.5 \times 10^7 \text{ M}^{-1} \text{ s}^{-1}$ ) and imidazole ( $2 \times 10^7 \text{ M}^{-1} \text{ s}^{-1}$ ) are almost comparable [24]. Hence the rate of RNO bleaching should be reduced to 50% if equal concentration of imidazole and DABCO are used. In the present study, the experiments were carried out in the presence of 10 mM imidazole and 5 mM DABCO. Hence bleaching rate was decreased by about 25%, when compared to the rate in the absence of DABCO (Fig. 4). Similarly, sodium azide, another  $^1\text{O}_2$  quencher also was used. The concentrations of sodium azide and imidazole used were 0.1 and 10 mM, respectively. At these concentrations, the RNO bleaching was inhibited by 50%, confirming the generation of  $^1\text{O}_2$  during photodynamic process.

It is known that RNO is also bleached by OH radicals formed through a non-Type II mechanism [25]. The hydroxyl radical can be generated from  $\text{O}_2^{\bullet-}$  via the metal catalyzed Fenton reaction as shown in the following scheme [26].



The contribution of OH radicals to RNO bleaching could be minimized by using metal chelates such as DETAPAC and EDTA, which render the metal ion redox inactive. However, since both their chelators could participate in electron transfer reactions with the excited sensitizer molecules this could lead to additional difficulties. Addition of (50  $\mu\text{g}/\text{ml}$ ) SOD and

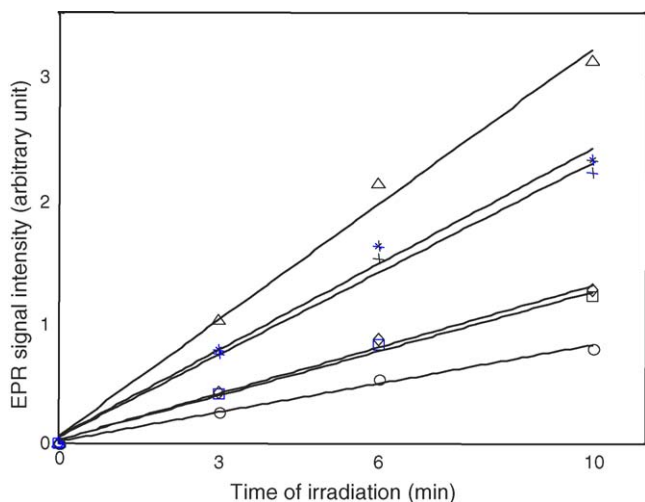


Fig. 5. EPR signal intensity of TEMPOL formed during the photoirradiation of solutions containing AC1 ( $\Delta\Delta\Delta$ ), AC2 (xxx), AC3 ( $\square\square\square$ ), AC4 (ooo), AC5 ( $\diamond\diamond\diamond$ ) and AC6 (\*\*\*) in the presence of TEMPL (20 mM) at 300 K in DMSO. EPR spectrometer settings: microwave power, 2 mW; modulation frequency, 100 kHz; modulation amplitude, 1 G; time constant, 0.1 s; scan rate, 4 min; scan width, 200 G.

catalase, which remove  $O_2^{\bullet-}$  and  $H_2O_2$  from the reaction mixture, respectively permits the detection and quantification of  $^1O_2$  without interference from OH radical.

EPR–TEMPL method was also used to investigate the photogeneration of  $^1O_2$  by 3-arylcoumarins in the presence of air. When a reaction mixture of TEMPL and 3-arylcoumarins was irradiated, an EPR spectrum of three equal intensity lines, characteristic of nitroxide radical (TEMPOL) was detected. The hyperfine splitting constant ( $A_N = 15.6$  G) was found to be identical with those of the authentic sample of TEMPOL. EPR signal intensity of TEMPOL produced was found to increase with increase of irradiation time, as shown in Fig. 5 for 3-arylcoumarins. Control experiments indicated that 3-arylcoumarin, oxygen and light were all essential for the production of TEMPOL. Comparative studies between 3-arylcoumarin and the well known  $^1O_2$  sensitizer, RB indicated that 3-arylcoumarins are moderate  $^1O_2$  generators. From Fig. 5, the  $^1O_2$  generating ratios of RB, AC1, AC6, AC2, AC5, AC3 and AC4 were determined to be 1:0.15:0.11:0.10:0.06:0.06:0.04. The rates of formation of TEMPOL by 3-arylcoumarins are parallel to their  $^1O_2$  generating quantum yields measured by RNO bleaching method. To confirm the generation of  $^1O_2$ , experiments were also carried out in the presence of specific singlet oxygen quencher such as sodium azide. The addition of sodium azide decreases the EPR signal intensity of the adduct confirming the photogeneration of  $^1O_2$ .

### 3.1.2. Electron transfer process

The photogeneration of  $O_2^{\bullet-}$  was studied by following the ferricytochrome *c* reduction efficiencies. The rate of cytochrome *c* reduction in air-saturated solution of the 3-arylcoumarins was observed in the presence of cytochrome *c* (40  $\mu$ M) and phosphate buffer (pH 7.4) DMSO (10%) solution. 3-Arylcoumarins AC1–AC6 were found to reduce cytochrome *c* with moderate

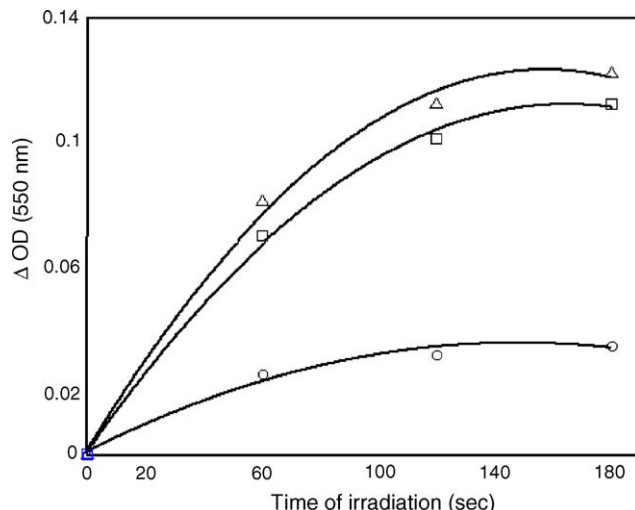


Fig. 6. Photosensitised cytochrome *c* reduction in 50 mM phosphate buffer, pH 7.4 by AC6 ( $\circ\circ\circ$ ), AC6 + EDTA ( $\Delta\Delta\Delta$ ) and AC6 + DETAPAC ( $\square\square\square$ ).

efficiencies. The rates of superoxide anion generation by AC1, AC2, AC3, AC4, AC5 and AC6 were derived to be 0.003, 0.001, 0.010, 0.037, 0.014 and 0.024  $\mu$ M/s, respectively. Fig. 6 shows the increase in absorbance at 550 nm with time of irradiation by AC6, and in the presence of electron donors. The rate of photoreduction is enhanced in the presence of electron donors such as EDTA and DETAPAC. Enhancement of generation of  $O_2^{\bullet-}$  in the presence of electron donor is indicative of anionic properties of radical intermediate formed during photosensitisation [27].

Generation of  $O_2^{\bullet-}$  from 3-arylcoumarins was confirmed by EPR spin trapping experiment using DMPO as the spin trap. DMPO-spin trapping has been successfully applied to trap radical intermediates, especially  $O_2^{\bullet-}$  and  $\bullet$ OH, because it has high affinity for reactive radicals and leads to the formation of stable spin adducts. The lifetime of DMPO- $O_2^{\bullet-}$  adduct is short in protic solvent such as water. Hence, the EPR spin-trapping studies were carried out in DMSO in which the DMPO- $O_2^{\bullet-}$  adduct has a longer lifetime [28]. EPR signal was not observed when DMPO alone was irradiated, or in dark, or in the absence of  $O_2$  (Fig. 7A). However, multiline EPR spectra were obtained when the coumarins were photolysed in the presence of DMPO (100 mM) in air-saturated DMSO solution (Fig. 7B). The observed EPR spectrum could be readily analysed in terms of a mixture of two type of spin adducts. Hyperfine coupling constants (hfcc) for one of the spin adduct were arrived at as a primary nitrogen triplet ( $A_N = 13.0$  G) split by a proton ( $A_H^\beta = 10.8$  G) which in turn is further split by a secondary proton ( $A_H^\gamma = 1.2$  G). The hfccs of the other spin adduct are  $A_N = 13.7$  G and  $A_H^\beta = 12.3$  G. These spectra could be readily assigned to DMPO- $O_2^{\bullet-}$  and DMPO-OH, respectively according to the reported values [29,30]. EPR spectra of these two spin adducts were computer simulated separately with their corresponding hfcc values. When these two computer simulated spectra were combined in the ratio of 2.5:7.5 for  $O_2^{\bullet-}$  and  $\bullet$ OH, respectively, the simulated EPR spectrum (Fig. 7C) matched well with the experimentally observed one. Formation of DMPO- $O_2^{\bullet-}$  adduct was also confirmed by the addition of SOD (50  $\mu$ g/ml)

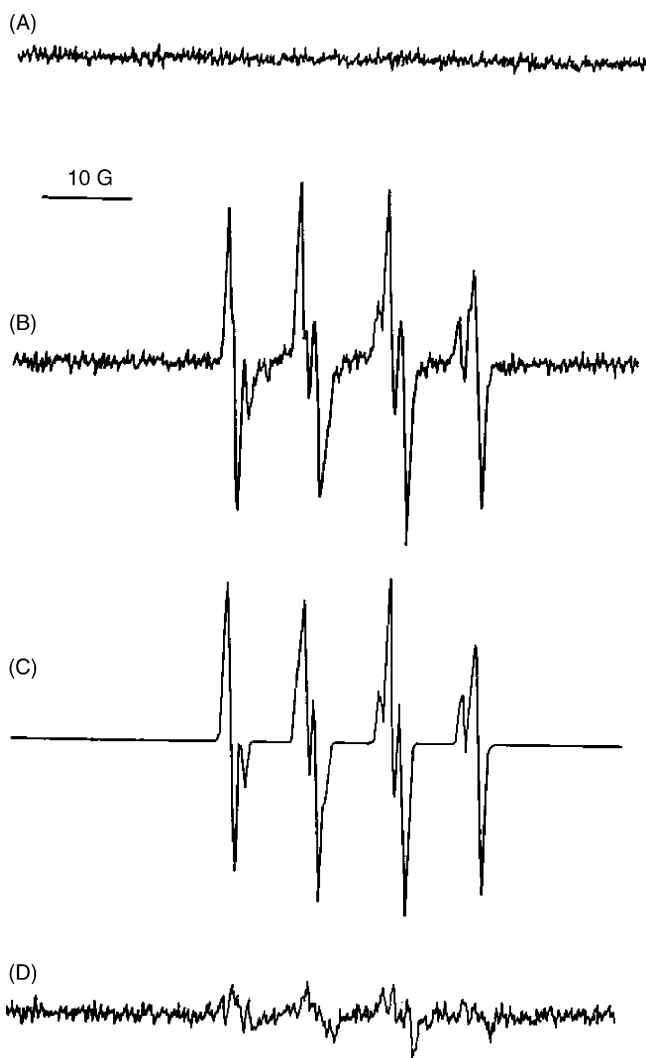


Fig. 7. EPR spectra from system containing AC1 (0.4 mM), DMPO (100 mM) in air-saturated DMSO: (A) in dark, (B) after 4 min irradiation, (C) simulated EPR spectrum, the spectrum contains two spin adducts: DMPO- $O_2^{\bullet-}$  ( $A_N = 13.0$  G,  $A_H^\beta = 10.8$  G,  $A_H^\gamma = 1.2$  G) and DMPO-OH adduct ( $A_N = 13.7$  G and  $A_H^\beta = 12.3$  G) in the ratio of 2.5: 7.5, (D) in the presence of SOD (50  $\mu$ g/ml). Instrumental settings: microwave power, 2 mW; modulation frequency, 100 kHz; modulation amplitude, 0.5 G; time constant, 0.1 s; scan rate, 4 min, scan range, 200 G and receiver gain, 500.

prior to illumination which inhibited the generation of spin adduct, Fig. 7D. This suggests a role of the superoxide ion in the production of the DMPO-OH adduct [31–33].

Similarly, multiline EPR spectra were observed for another coumarin AC5. Hyperfine coupling constant values for one of the spin adduct ( $A_N = 12.8$  G,  $A_H^\beta = 10.5$  G and  $A_H^\gamma = 1.3$  G) and the other spin adduct was ( $A_N = 13.8$  G and  $A_H^\beta = 12.1$  G) readily assigned to DMPO- $O_2^{\bullet-}$  and DMPO-OH, respectively, according to the reported values [30,34] (figure not shown).

### 3.2. Photodynamic action of flavanocoumarins

#### 3.2.1. Energy transfer process

The rate of bleaching of RNO as a function of illumination time is shown in Fig. 8 for the flavanocoumarin. The  $^1O_2$  yield

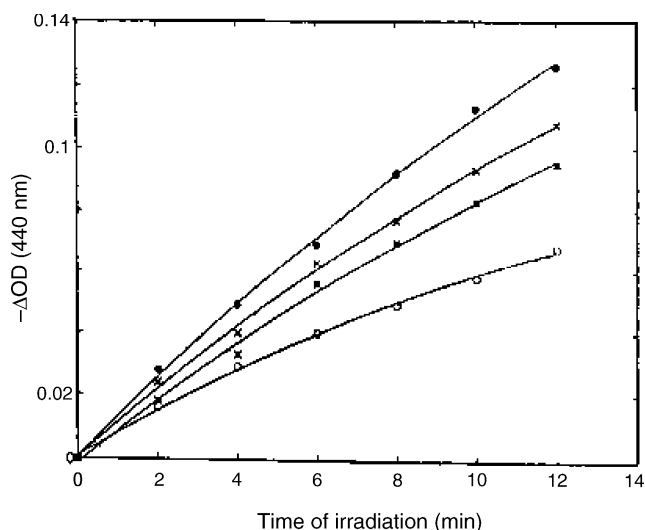


Fig. 8. Photosensitized RNO bleaching, measured at 440 nm in the presence of imidazole (10 mM) in 50 mM phosphate buffer (pH 7.4), by FC I (ooo), FC II (\*\*\*) , FC III (●●●) and FC IV (xxx), as a function of illumination time.

was calculated as similar to the 3-arylcoumarins. The relative yields thus calculated are, 0.04, 0.03, 0.10 and 0.06 for FC I, FC II, FC III and FC IV respectively, taking  $\Phi(^1O_2)$  of RB = 0.76. 3-arylcoumarins show saturated behaviour in  $^1O_2$  yield. Flavanocoumarins does not show any saturated behaviour perhaps be due to the extensive conjugation of flavanocoumarin than 3-arylcoumarins.

The spin trapping of  $^1O_2$  by TEMPL was used as an alternative method to determine the formation of  $^1O_2$  by flavanocoumarins. The rate of formation of the TEMPOL by these sensitizers is parallel to their  $^1O_2$  generating efficiencies. To confirm the generation of  $^1O_2$ , experiments were also carried out in the presence of specific singlet oxygen quencher such as sodium azide (figure not shown). The almost same singlet oxygen generation efficiencies of 3-arylcoumarins and flavanocoumarins may be due to the same energy transfer to the dissolved  $O_2$  molecule. There is no relationship noticed between the chemical structure of coumarins and  $^1O_2$  generating efficiencies as similar to quinones. This may be due to some other photo physical process occurring during the photosensitisation of coumarin derivatives.

#### 3.2.2. Electron transfer process

Generation of  $O_2^{\bullet-}$  from flavanocoumarins on photoillumination, could be readily studied by following the ferricytochrome *c* reduction efficiencies. Fig. 9 shows the rates of ferricytochrome *c* reduction when air saturated solutions of flavanocoumarin are photolysed in the presence of 40  $\mu$ M cytochrome *c* in 50 mM phosphate buffer solution. The rates of superoxide anion generation by FC I, FC II, FC III and FC IV were calculated to be 0.035, 0.033, 0.030 and 0.044  $\mu$ M/s, respectively.

The DMPO spin trapping method was also employed to investigate the formation of  $O_2^{\bullet-}$  by flavanocoumarins. Fig. 10 shows the EPR spectrum for FC1. The observed EPR spectrum contains components from two DMPO spin adducts. Hyperfine coupling of one of the spin adducts was analysed as follows:  $A_N = 13.8$  G,

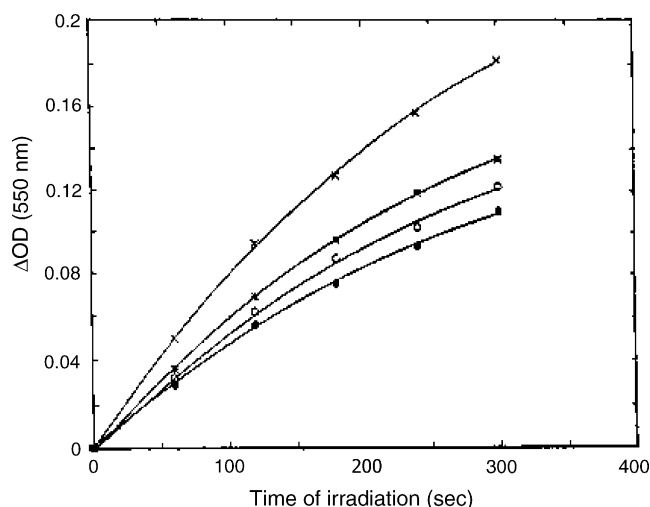


Fig. 9. Photosensitised cytochrome *c* reduction in 50 mM phosphate buffer, pH 7.4 by FC I (○ ○ ○), FC II (\*\*\*) , FC III (● ● ●) and FC IV (xxx).

$A_H^\beta = 11.3$  G and  $A_H^\gamma = 1.3$  G. For the other spin adduct, the hfcc's are:  $A_N = A_H^\beta = 14.4$  G. These two spin adducts could be readily identified as DMPO- $O_2^{\bullet-}$  and DMPO-OH adduct respectively. The simulated EPR spectra were combined in the ratio of 8:2 for  $O_2^{\bullet-}$  and  $\bullet OH$  respectively, and found to match well with the experimentally observed one (Fig. 10c). The addition of SOD prior to irradiation eliminated the spectrum of DMPO- $O_2^{\bullet-}$  and the four line pattern characteristic of DMPO-OH adduct could be very clearly seen (Fig. 10d). FC II also exhibited similar behaviour showing the formation of both  $O_2^{\bullet-}$  and  $\bullet OH$ . However, the four-line pattern was not seen when FC III and FC IV were photolysed. Studying the effect of SOD, which is an effective scavenger of  $O_2^{\bullet-}$ , provided further support for the generation of these two species.

The formation of DMPO-OH adduct can be explained by three possible ways [35] such as: (i) generation of free  $\bullet OH$ ; (ii) decay of DMPO- $O_2^{\bullet-}$  signal to DMPO-OH; (iii) formation of complex between DMPO and  $^1O_2$  and its subsequent decay to DMPO-OH. Singlet oxygen mediated oxidation of DMPO to  $\bullet OH$  radical species is also well documented [36–38]. Reaction of  $^1O_2$  with DMPO is reported to give a complex followed by decay to DMPO-OH and free  $\bullet OH$  which might be trapped by DMPO.

The possible involvement of  $^1O_2$  in the generation of DMPO-OH adduct can be tested by performing a competition experiment with a  $^1O_2$  scavenger such as sodium azide. During the photolysis of FC I in the presence of DMPO and sodium azide, EPR spectrum shown in Fig. 11a was observed. When the simulated EPR spectra of two spin adducts were combined, the simulated spectrum matched with the experimentally observed one (Fig. 11b). Hyperfine coupling constant values of one of the spin adducts were  $A_N = 12.8$  G,  $A_H^\beta = 10.4$  G and  $A_H^\gamma = 1.4$  G. For the other spin adduct, the hfccs are  $A_{N1} = 13.8$  G,  $A_H^\beta = 14.0$  G and  $A_{N2} = 3.1$  G. These two adducts may be identified as DMPO- $O_2^{\bullet-}$  and DMPO- $N_3^\bullet$  respectively, based on the literature values [39]. It is well known that azide anion can interact with  $\bullet OH$  to generate  $N_3^\bullet$ , which may then be trapped by DMPO [40].

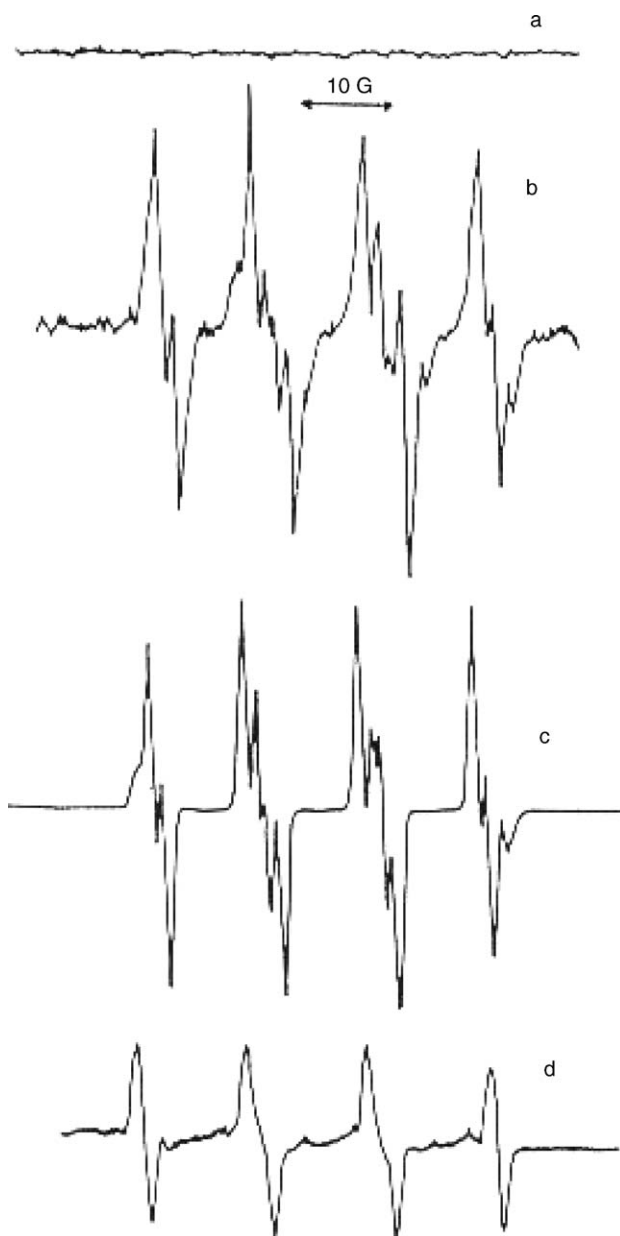


Fig. 10. EPR spectra observed during irradiation of FC I (280  $\mu M$ ) in the presence of DMPO (100 mM) in air saturated DMSO solution: (a) in dark, (b) after 5 min irradiation, (c) simulated EPR spectrum obtained by the summation of two spin adducts using hfcc's values:  $A_N = 13.8$  G,  $A_H^\beta = 11.3$  G,  $A_H^\gamma = 1.3$  G for DMPO- $O_2^{\bullet-}$  adduct and  $A_N = A_H^\beta = 14.4$  G for DMPO-OH, (d) after 5 min irradiation in the presence of SOD showing four line pattern of DMPO-OH. Instrumental settings: same as in Fig. 7.

Hence it may be concluded that singlet oxygen is not involved in the photosensitised production of  $\bullet OH$ . The above observation clearly confirms the formation of free  $\bullet OH$  radical during the photolysis of FC I.

The relative photogeneration efficiencies of  $^1O_2$  and  $O_2^{\bullet-}$  by 3-arylcoumarins and flavanocoumarins are analysed. The chemical structure/ROS generating efficiency study of the coumarins showed that the presence of electron donating substituents on the coumarin ring enhances their  $O_2^{\bullet-}$  generating efficiencies. The presence of coumarin and chromone in a single system (fla-

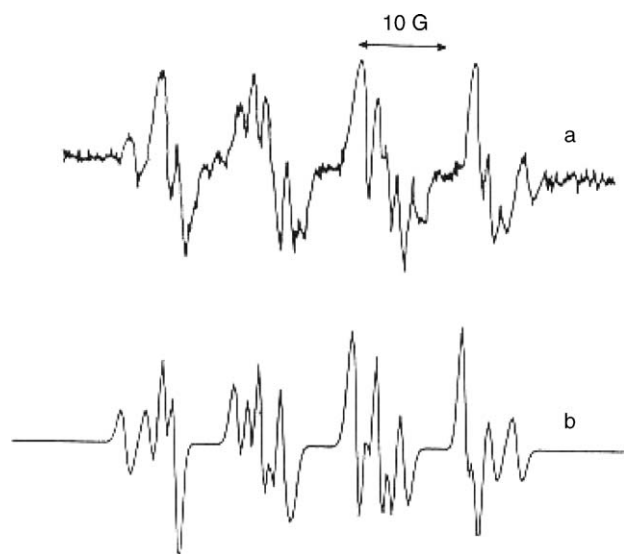


Fig. 11. (a) EPR spectra observed during irradiation of FC I and DMPO in the presence of sodium azide in DMSO. (b) Computer simulated spectrum obtained by the summation of two spin adducts using hfcc's values:  $A_{N1} = 14.8$  G,  $A_{H1}^{\beta} = 14.4$  G,  $A_{N2} = 3.1$  G for DMPO- $N_3^{\bullet}$  adduct,  $A_N = 13.8$  G,  $A_{H1}^{\beta} = 11.0$  G,  $A_{H1}^{\gamma} = 1.3$  G for DMPO- $O_2^{\bullet-}$  adduct. Instrumental settings: same as in Fig. 7.

vanocoumarin) enhanced the  $O_2^{\bullet-}$  generation efficiencies than the 3-arylcoumarin system.

Based on the result obtained from RNO bleaching, EPR-TEMPL, SOD-inhibitable cytochrome *c* reduction and EPR spin trapping experiments, it may be concluded that the reactive oxygen species such as  $O_2^{\bullet-}$ ,  $^1O_2$  and  $\bullet OH$  are formed during the photolysis of 3-arylcoumarins and flavanocoumarins. These observations indicate that both electron transfer (Type I) and energy transfer (Type II) are involved in the photosensitisation process of 3-arylcoumarins and flavanocoumarins.

## Acknowledgements

We thank Chemistry Department, Pondicherry University, Pondicherry, for EPR measurements. Thanks are due to UGC, New Delhi for the award of a teacher fellowship and to the Managing Board, N.M.S.S.V.N. College, Madurai, Tamilnadu, India for study leave to M.R. Support from UGC as center for Potential in Genomics Science Programme is also gratefully acknowledged.

## References

[1] R.D. Murray, J. Mendez, S.A. Bron, *The Natural Coumarins*, John Wiley & Sons, Chichester, 1982.

- [2] O.S. Sione, *J. Pharmaceut. Sci.* 53 (1964) 231.  
 [3] J.W.T. Selway, in: V. Cody, E. Middleton, J.B. Harborne (Eds.), *Plant Flavonoids in Biology and Medicine*, Alian Liss, New York, 1986, p. 521.  
 [4] D.A. Smith, W. Banks, *Phytochemistry* 25 (1986) 979.  
 [5] D.C. Opdyku, *Dragoco Report* 2, 1981, p. 42.  
 [6] R.S. Becker, S. Chakravorti, C.A. Garter, *J. Chem. Soc. Faraday Trans.* 89 (1993) 1007.  
 [7] N.K. Gibbs, E. Quanten, S. Baydoren, C.N. Knox, R. Roerandt, F. De Schryver, T.G. Truscott, A.R. Young, *J. Photochem. Photobiol. B: Biol.* 2 (1988) 109.  
 [8] C. Salet, G. Moreno, F. Vinzens, *Photochem. Photobiol.* 36 (1982) 291.  
 [9] A. Potapenko, *J. Photochem. Photobiol. B: Biol.* 9 (1991) 1.  
 [10] H. Singh, J.A. Vadasz, *Photochem. Photobiol.* 28 (1978) 539.  
 [11] A.Ya. Potapenko, *J. Photochem. Photobiol. B.* 9 (1991) 1.  
 [12] N.J. De Mol, G.M.J. Beijersbergen, V. Henegoumen, B. Weeda, C.W. Knox, T.G. Truscott, *Photochem. Photobiol.* 44 (1986) 747.  
 [13] B. Kalyanaraman, C.C. Felix, R.C. Sealy, *Photochem. Photobiol.* 36 (1982) 5.  
 [14] A. Vanangamudi, R. Gandhidasan, P.V. Raman, *J. Indian, Heterocyclic Chem.* 7 (1997) 85.  
 [15] I. Kraljic, S. El Mohsni, *Photochem. Photobiol.* 28 (1978) 577.  
 [16] J. Johnson Inbaraj, R. Gandhidasan, R. Murugesan, *J. Photochem. Photobiol. Chem. A* 124 (1999) 95–99.  
 [17] E. Gandin, Y. Lion, *J. Photochem.* 20 (1982) 77.  
 [18] P.C.C. Lee, A.J. Rodgers, *Photochem. Photobiol.* 45 (1987) 79.  
 [19] J.M. McCord, I. Fridovich, *J. Biol. Chem.* 244 (1969) 6049.  
 [20] W.H. Koppenol, J. Butler, *Isr. J. Chem.* 24 (1984) 11.  
 [21] Y. Lion, M. Demelle, A. Van De Vorst, *Nature* 263 (1976) 442.  
 [22] J. Moan, E. World, *Nature* 279 (1979) 450.  
 [23] E. Gandin, Y. Lion, *J. Photochem. Photobiol.* 20 (1982) 77.  
 [24] F. Wilkinson, J.G. Brummer, *J. Phys. Chem. Ref. Data* 10 (1981) 809.  
 [25] W. Bors, C. Michel, M. Saran, *Eur. J. Biochem.* 95 (1979) 621.  
 [26] H.C. Sutton, G.F. Vile, C.C. Winterbourn, *Arch. Biochem. Biophys.* 256 (1987) 462.  
 [27] Z. Diwu, *Free Radic. Biol. Med.* 14 (1993) 209.  
 [28] E. Ben-Hur, A. Carmichael, P. Riesz, I. Rosenthal, *Int. J. Radiat. Biol.* 48 (1985) 837.  
 [29] T. Ozawa, A. Hanaki, *Chem. Pharm. Bull.* 26 (1978) 2572.  
 [30] B. Kalyanaraman, C. Mottley, R.P. Mason, *J. Biochem. Biophys. Meth.* 9 (1984) 27.  
 [31] A. Samuni, M.C. Krishna, P. Riesz, E. Finkelstein, A. Russo, *Free Radic. Biol. Med.* 6 (1989) 141.  
 [32] A.J. Carmichael, M.M. Mossoba, P. Riesz, *FEBS Lett.* 164 (1983) 401.  
 [33] E. Finkelstein, G.M. Rosen, E.J. Rauchman, J. Paxton, *Mol. Pharmacol.* 16 (1979) 676.  
 [34] J.J. Inbaraj, M.C. Krishna, R. Gandhidasan, R. Murugesan, *Biochim. Biophys. Acta* 1472 (1999) 462.  
 [35] J. Felix, B. Kalyanaraman, *Arch. Biochem. Biophys.* 15 (1991) 43.  
 [36] P. Bilsky, K. Reszka, M. Bilaska, C. Chignell, *J. Am. Chem. Soc.* 118 (1996) 1330.  
 [37] M. Collet, M. Hoebeke, J. Pipette, A. Van de Vorst, A. Jakobs, L. Lindqvist, *J. Photochem. Photobiol. B: Biol.* 99 (1996) 1.  
 [38] G. Buttner, *Free Radic. Res. Commun.* 19 (1993) 79.  
 [39] K. Reszka, D. Kolodziejczyk, J.W. Lown, *Free Radic. Biol. Med.* 5 (1988) 63.  
 [40] W. Kremers, A. Singh, *Can. J. Chem.* 58 (1980) 1592.